Quantum computing with nearest neighbor interactions and error rates over 1%

David S. Wang, Austin G. Fowler, Lloyd C. L. Hollenberg
Centre for Quantum Computer Technology, University of Melbourne, Victoria, Australia
(Dated: September 21, 2010)

Large-scale quantum computation will only be achieved if experimentally implementable quantum error correction procedures are devised that can tolerate experimentally achievable error rates. We describe a quantum error correction procedure that requires only a 2-D square lattice of qubits that can interact with their nearest neighbors, yet can tolerate quantum gate error rates over 1%. The precise maximum tolerable error rate depends on the error model, and we calculate values in the range 1.1–1.4% for various physically reasonable models. Even the lowest value represents the highest threshold error rate calculated to date in a geometrically constrained setting, and a 50% improvement over the previous record.

Building a quantum computer is a daunting task. Engineering the ability to interact nonlocal pairs of qubits is particularly challenging. All existing quantum error correction (QEC) schemes capable of tolerating error rates above 1% assume the ability to deterministically interact pairs of qubits separated by arbitrary distances with no time or error rate penalty [1–3]. The most recent of these works estimates a threshold error rate p_{th} of 5% [3].

It is far more physically reasonable to assume a 2-D lattice of qubits with only nearest neighbor interactions, proposed realizations of which exist for ion traps [4], optical lattices [5], superconducting qubits [6], optically addressed quantum dots [7, 8], NV centers in diamond [9] and many other systems. For such proposals, the leading QEC scheme [10, 11], which is based on the Kitaev surface code [12], has been shown to possess a p_{th} of 0.75% [10, 13, 14]. We increase this to 1.1–1.4%, depending on the error model, bringing the threshold for geometrically constrained quantum computing above 1% for the first time. We achieve this by carefully using the given error model to calculate approximate probabilities of different error events and removing the need to initialize qubits.

To overview, we will begin by describing stabilizers and our simplified quantum gate sequence, followed by a detailed discussion of how probable different error events are and how this information can be fed into the classical decoding algorithm. We then present the results of detailed simulations, which apply two-qubit depolarizing noise with probability p_2 after two-qubit quantum gates, single-qubit depolarizing noise with probability p_I after identity gates, and make use of measurement gates that report and project into the wrong eigenstate with probability p_M. In addition to the standard error model with $p_2 = p_I = p_M = p$, which we focus on, we simulate a balanced error model with $p_I = 4p_2/5$ and $p_M = 2p_I/3$, ensuring idle qubits have the same probability of error as a single qubit involved in a two-qubit gate and taking into account the fact that a measurement is only sensitive to errors in one basis. We also simulate the case $p_I = p_2/1000$ and $p_M = p_2/100$, modeling typical error ratios in an ion trap.

A stabilizer [15] of a state $|\Psi\rangle$ is an operator S such that $S|\Psi\rangle = |\Psi\rangle$. An error E that anticommutes with S can be detected as $SE|\Psi\rangle = -ES|\Psi\rangle = -E|\Psi\rangle$. Examples of surface code stabilizers [12] are shown in fig. 1a. Circuits measuring these stabilizers without explicit initialization gates are shown in fig. 2. We assume quantum nondemolition measurements, which have been experimentally demonstrated using ion traps [16], optical lattices [17], superconducting qubits [18] and NV centers in diamond [19] and theoretically proposed for optically addressed quantum dots [20, 21]. The initial and final measurements match when $+E$ is measured and differ when $-E$ is measured. An appropriate sequence of two-qubit gates for measuring all stabilizers across the lattice simultaneously is shown in fig. 1b. Data qubits execute identity gates while the syndrome qubits are measured.

Repeatedly executing the gates of fig. 1b, along with

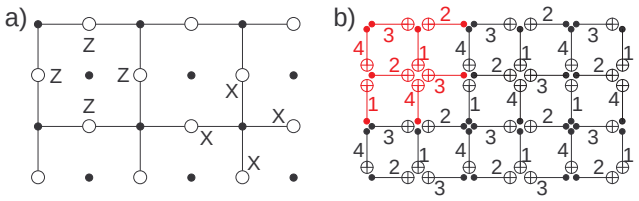

FIG. 1: a) 2-D lattice of data qubits (circles) and syndrome qubits (dots) and examples of the data qubit stabilizers. b) Sequence of CNOTs permitting simultaneous measurement of all stabilizers. Numbers indicate the relative timing of gates. The highlighted gates can be tiled to fill the plain.

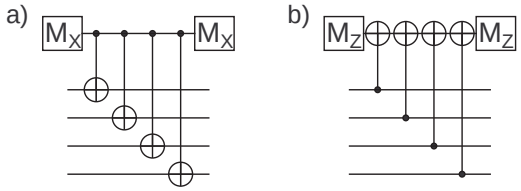

FIG. 2: Circuit determining the sign of a stabilizer a) $XXXX$, b) $ZZZZ$, without explicit initialization gates.

appropriate syndrome qubit measurements and data qubit identity gates, generates points in space and time where the stabilizer changes sign, indicating local errors. Renormalization techniques exist capable of processing perfect syndrome information [22, 23], however at present only the minimum weight perfect matching algorithm [24, 25] can be used to process the output of realistic quantum circuits.

The minimum weight perfect matching algorithm takes coordinates and a measure of separation and matches pairs of coordinates such that the total separation is a minimum. Chains of corrective operations connecting matched pairs can then be applied. Prior work has calculated the separation of two syndrome changes $s_1 = (i_1, j_1, t_1)$, $s_2 = (i_2, j_2, t_2)$ using $d(s_1, s_2) = |i_1 - i_2| + |j_1 - j_2| + |t_1 - t_2|$ [10, 13, 14], however it was shown in [26] that this is far from optimal and leads to poor performance, particularly at low error rates. In this work, we instead approximate the probability $P(s_1, s_2)$ of a given pair of syndrome changes being connected by an error chain, and set $d(s_1, s_2) = -\ln(P(s_1, s_2))$. This choice of $d(s_1, s_2)$ is natural, accounting for the substantial performance increase we observe.

To calculate $P(s_1, s_2)$, we must study the effect gate errors. Fig. 3 shows all possible pairs of syndrome changes resulting from all possible errors on all meaningfully distinct gates. The CNOTs shown measure an X-stabilizer. The effect of errors on the CNOTs used to measure a Z-stabilizer can be obtained by interchanging X and Z.

Using fig. 3, fig. 4 was constructed, grouping gate errors leading to specific pairs of syndrome changes. The probability of an odd number of errors occurring in each group gives the probability of the associated link. Using the standard error model, the probability of the link shown in fig. 4a is

$$p_A = \frac{16p}{15}\left(1 - \frac{4p}{15}\right)^3 (1-p) + p\left(1 - \frac{4p}{15}\right)^4 + O(p^3). \tag{1}$$

Defining similar probabilities p_B, p_C, p_D, p_E, p_F for fig. 4b–f, fig. 5 shows the $O(p)$ links from one syndrome to its neighbors. Some straightforward modifications of the links and expressions are required at the temporal and spatial boundaries.

The probability $P(s_1, s_2)$ that two syndrome changes are connected is the sum of the probabilities of all connecting paths. The probability of a given path is the product of the link probabilities along the path. Several approximations of $P(s_1, s_2)$ are worthy of study. The simplest approximation is to take a single path of maximum probability $P_{\max}(s_1, s_2)$ and define $d_{\max}(s_1, s_2) = -\ln(P_{\max}(s_1, s_2))$. We shall see that this approximation is sufficient to substantially increase p_{th}, and that more accurate approximations do not lead to further increase. The performance of surface code QEC using $d_{\max}(s_1, s_2)$ and the standard error model is shown in figs. 6–7.

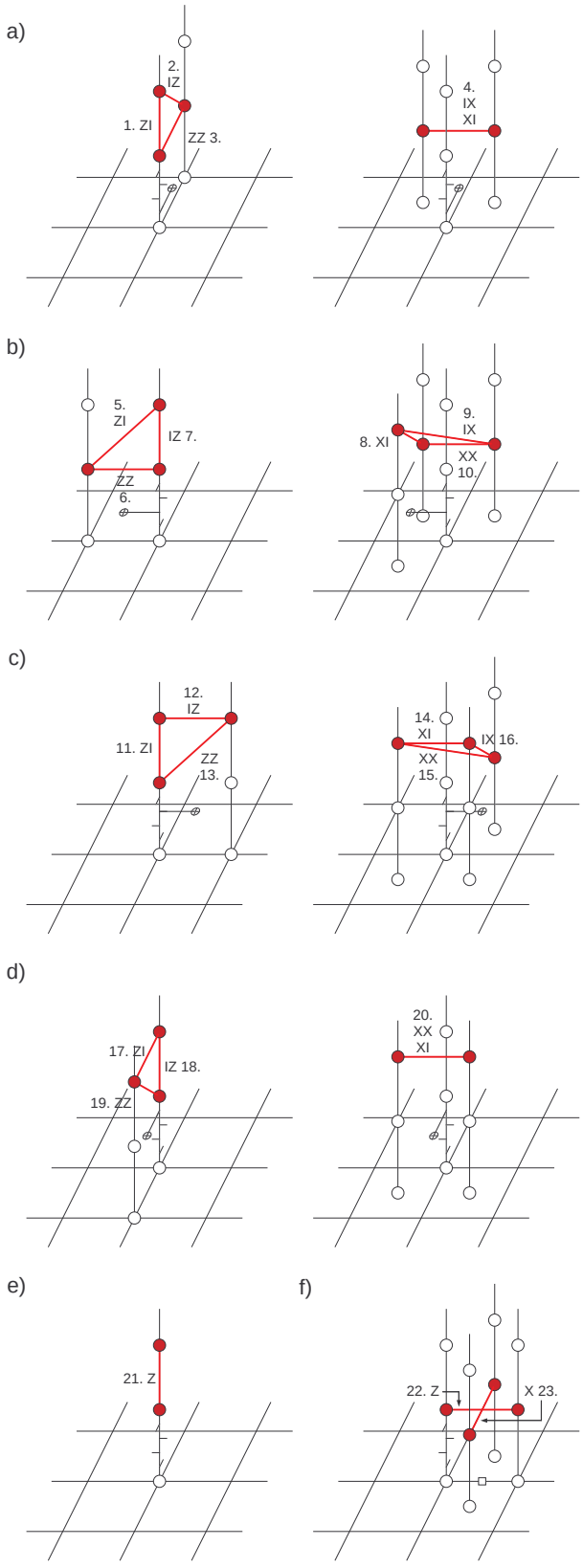

FIG. 3: Syndrome changes resulting from a-d) specific two-qubit errors on specific CNOTs, e) a syndrome qubit measurement error, f) a data qubit memory error.

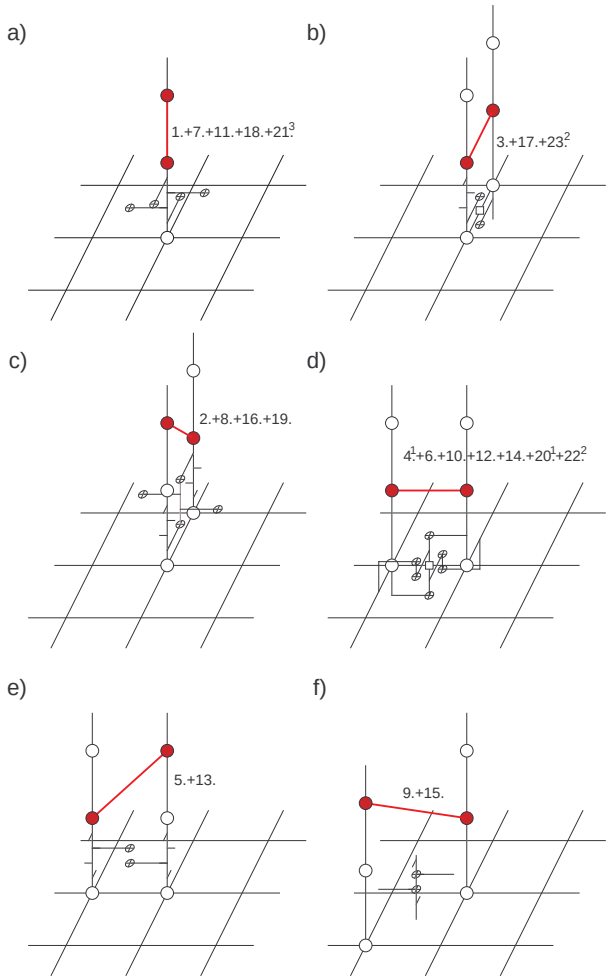

FIG. 4: Numbered error processes from fig. 3 contributing to specific links. Superscripts 1, 2 and 3 indicate errors occurring with probability $8p_2/15$, $2p_I/3$ and p_M respectively. All others occur with probability $4p_2/15$.

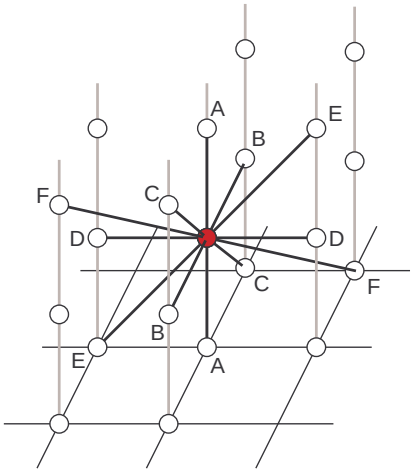

FIG. 5: All possible links from a syndrome change to its neighbors. Letters correspond to figs. 4a–f.

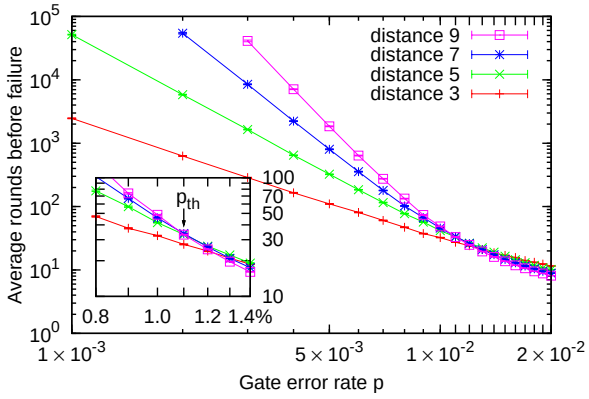

FIG. 6: Average rounds of error correction before logical X failure as a function of the gate error rate p when using $d_{\max}(s_1, s_2)$ and the standard error model.

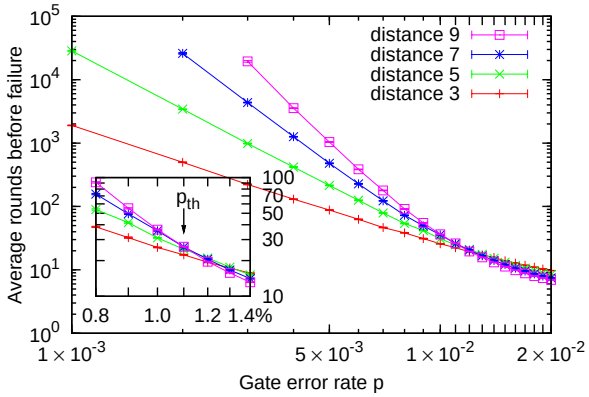

FIG. 7: Average rounds of error correction before logical Z failure as a function of the gate error rate p when using $d_{\max}(s_1, s_2)$ and the standard error model.

Figs. 6–7 give strong evidence of $p_{\text{th}} = 1.1\%$. We have verified this by simulating high distance codes at $p = 1.1\%$ and observing neither increase nor decrease of the failure time. This is enormously encouraging, and motivates one to better approximate $P(s_1, s_2)$ in an effort to further increase p_{th}. Additional accuracy can be achieved by taking all shortest length paths (measured in links) between s_1 and s_2 and calculating the sum of products of link probabilities along each path. We shall define the resulting distance measure as $d_0(s_1, s_2)$. We can define similar distance measures $d_n(s_1, s_2)$ taking into account all minimum length l paths and paths of length no greater than $l+n$. The performance of surface code QEC around p_{th} using $d_0(s_1, s_2)$ is shown in fig. 8. It can be seen that p_{th} remains 1.1%.

The fact that d_0 results in the same p_{th} as using a single maximum probability path distance measure $d_{\max}$ can be explained by noting that $d_0(s_1, s_2)$ only differs from

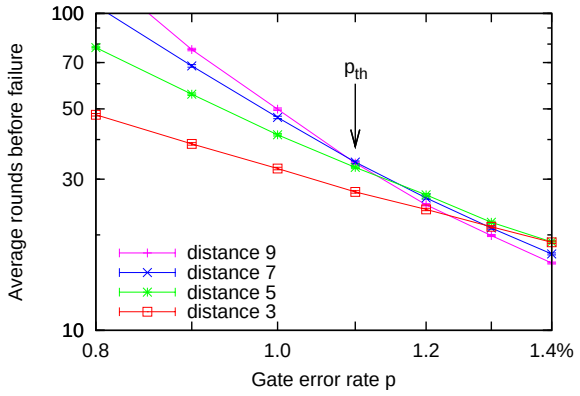

FIG. 8: Average rounds of error correction before logical X failure as a function of the gate error rate p when using $d_0(s_1, s_2)$ and the standard error model. $p_{\rm th}$ remains 1.1%.

$d_{\rm max}(s_1, s_2)$ if s_1, s_2 are separated by at least two links. Single link paths are unique minimum length paths implying $d_0 = d_{\rm max}$. The vast majority of error chains, even for $p = p_{\rm th}$, are single links. We find that the modification of the distance associated with the multiple paths of syndrome changes separated by multiple links is in the region of 10–20%. Given such multiple link paths are not leading order contributors to $p_{\rm th}$ in the first place, this relatively small weight change does not result in an observable improvement of $p_{\rm th}$.

Higher order approximations $d_n(s_1, s_2)$ will also result in the same $p_{\rm th}$ as the distance is hardly altered by increasing n. To take a typical example, for $p = 0.01$, $s_1 = (0, 0, 0)$, $s_2 = (1, -1, 0)$ we obtain $d_0 = 6.91$ (6 paths), $d_1 = 6.86$ (30 paths) and $d_2 = 6.85$ (390 paths). The exponential increase of the number of paths is well balanced by the exponential decrease of the probability of these paths.

The balanced error model is a better model of all quantum gates failing with equal probability than the standard error model, and appropriate modification of the polynomials using $p_2 = p$, $p_I = 4p/5$ and $p_M = 8p/15$ leads to $p_{\rm th} = 1.2\%$. The ion trap error model, with $p_2 = p$, $p_I = p/1000$ and $p_M = p/100$ leads to $p_{\rm th} = 1.4\%$. Arbitrary stochastic error models are straightforward to analyze using our formalism.

To conclude, by performing a detailed study of the probability of different pairs of syndrome changes and feeding the simplest approximation of this information into the minimum weight perfect matching algorithm, we have been able to raise the geometrically constrained threshold error rate to 1.1–1.4%, depending on the exact error model, while maintaining computational efficiency. This is the first time a geometrically constrained threshold error rate has been observed over the 1% level. There is the potential for still further improvement by taking into account correlations between X and Z errors, which shall be pursued in further work.

We acknowledge support from the Australian Research Council, the Australian Government, and the US National Security Agency (NSA) and the Army Research Office (ARO) under contract W911NF-08-1-0527.

[1] E. Knill, Nature **434**, 39 (2005), quant-ph/0410199.
[2] K. Fujii and K. Yamamoto, Phys. Rev. A **81**, 042324 (2010), arXiv:0912.5150.
[3] K. Fujii and K. Yamamoto, arXiv:1008.2048 (2010).
[4] R. Stock and D. F. V. James, Phys. Rev. Lett. **102**, 170501 (2009), arXiv:0808.1591.
[5] D. Jaksch, Contemporary Physics **45**, 367 (2004), quant-ph/0407048.
[6] D. P. DiVincenzo, arXiv:0905.4839 (2009), Nobel Symposium on Qubits for Quantum Information.
[7] R. Van Meter, T. D. Ladd, A. G. Fowler, and Y. Yamamoto, Int. J. Quantum Inf. **8**, 295 (2010), arXiv:0906.2686.
[8] N. C. Jones, R. Van Meter, A. G. Fowler, P. L. McMahon, J. Kim, T. D. Ladd, and Y. Yamamoto (2010), in preparation.
[9] N. Yao, L. Jiang, A. V. Gorshkov, P.Maurer, G. Giedke, J. I. Cirac, and M. D. Lukin (2010), in preparation.
[10] R. Raussendorf and J. Harrington, Phys. Rev. Lett. **98**, 190504 (2007), quant-ph/0610082.
[11] R. Raussendorf, J. Harrington, and K. Goyal, New J. Phys. **9**, 199 (2007), quant-ph/0703143.
[12] S. B. Bravyi and A. Y. Kitaev, quant-ph/9811052 (1998).
[13] A. G. Fowler, A. M. Stephens, and P. Groszkowski, Phys. Rev. A **80**, 052312 (2009), arXiv:0803.0272.
[14] D. S. Wang, A. G. Fowler, A. M. Stephens, and L. C. L. Hollenberg, Quant. Info. Comp. **10**, 456 (2010), arXiv:0905.0531.
[15] D. Gottesman, Ph.D. thesis, Caltech (1997), quant-ph/9705052.
[16] A. H. Burrell, D. J. Szwer, S. C. Webster, and D. M. Lucas, Phys. Rev. A **81**, 040302(R) (2010), arXiv:0906.3304.
[17] J. Kruse, C. Gierl, M. Schlosser, and G. Birkl, Phys. Rev. A **81**, 060308(R) (2010), arXiv:1001.3430.
[18] A. Lupascu, E. F. C. Driessen, L. Roschier, C. J. P. M. Harmans, and J. E. Mooij, Phys. Rev. Lett. **96**, 127003 (2006), cond-mat/0601634.
[19] F. Jelezko, T. Gaebel, I. Popa, M. Domhan, A. Gruber, and J. Wrachtrup, Phys. Rev. Lett. **93**, 130501 (2004), quant-ph/0402087.
[20] J. Berezovsky, M. H. Mikkelsen, O. Gywat, N. G. Stoltz, L. A. Coldren, and D. D. Awschalom, Science **314**, 1916 (2006).
[21] M. Atatüre, J. Dreiser, A. Badolato, and A. Imamoglu, Nature Physics **3**, 101 (2007), quant-ph/0610110.
[22] G. Duclos-Cianci and D. Poulin, Phys. Rev. Lett. **104**, 050504 (2010), arXiv:0911.0581.
[23] G. Duclos-Cianci and D. Poulin, arXiv:1006.1362 (2010).
[24] J. Edmonds, Canad. J. Math. **17**, 449 (1965).
[25] J. Edmonds, J. Res. Nat. Bur. Standards **69B**, 125 (1965).
[26] A. G. Fowler, D. S. Wang, and L. C. L. Hollenberg, arXiv:1004.0255 (2010).